Noncovalent Interactions

DOI: 10.1002/anie.201210365

Nanomechanics of Cation–π Interactions in Aqueous Solution**

Qingye Lu, Dongyeop X. Oh, Youngjin Lee, Yongseok Jho, Dong Soo Hwang, and Hongbo Zeng**

One type of important noncovalent interactions in biological systems is the cation–π interaction that is widely present between an electron-rich π system (e.g., Phe, Tyr, and Trp) and adjacent cations (e.g., Na^+ and K^+) or species containing positive charges (e.g., Lys and Arg) under physiological conditions of living organisms.[1] Electrostatic forces are the dominant components of cation–π interactions.[1g] Interestingly, the aqueous cation–π interaction is known to be stronger than an electrostatically driven salt bridge (the strongest noncovalent interaction in air) because of its low desolvation penalty.[1h] The hydrophobic aromatic ring selectively binds cations according to the degree of cation hydration, thus the cation–π interaction is vital to physiological activities[1i] such as potassium channel blocking by tetraethylammonium (TEA),[2] nicotinic acetylcholine (ACh) receptor binding,[3] protein folding,[4] T-cell antigen receptor binding,[5] and adhesion of mussel proteins to underwater surfaces.[6] Potassium channels are composed of membrane proteins that allow rapid and selective flow of K^+ ions across the lipid bilayer of the cell membrane, thereby suppressing the electrical activity in nerves and muscles as well as regulating the salt concentration in metabolism and digestion.[2] TEA inhibits the flow of potassium ions across the channel through cation–π binding with aromatic residues at the channel entrance.[2] The nicotinic acetylcholine receptor (nAChR) is a ligand-gated ion channel in the plasma membranes of certain neurons and on the postsynaptic side of the neuromuscular junction.[3] It is believed that cation–π interactions between the quaternary ammonium group of ACh and tryptophan residues of nAChR contribute strongly to the receptor mechanism.[3] Recently, it has been revealed that cation–π interactions also strongly contribute to underwater adhesion of mussel-foot proteins,[6] which lack negatively charged residues but have abundant aromatic and positively charged residues. Because of the important roles in biophysics and biochemistry, cation–π interactions in aqueous media have been investigated through both qualitative and quantitative approaches, specifically stoichiometric and spectral evidence for the presence of cation–π interactions in the aqueous phase using ^1H NMR spectroscopy,[7] voltage jump,[8] UV/Vis, and resonance Raman spectroscopy,[9] and extensive computational studies of metal ion–small molecule complexes.[1a,f,h,j–l] However, the nanomechanics of cation–π interactions in aqueous solution has not been directly evaluated by mechanical force techniques.

Herein, the mechanical nature of cation–π interactions in aqueous media was probed directly using a surface forces apparatus (SFA) for the first time. Special attention was paid to the impact of the cation type and concentration and the type of aromatic side group present. SFA is a technique that has been widely applied to measure forces (F) between two surfaces as a function of separation distance (D) in various vapors or liquids.[10] In this work, a model system was built to measure the cation–π interaction in aqueous solutions. Briefly, one surface was coated with positively charged poly-L-lysine (PLL) (primary amine, NH_3R^+) and another surface was coated with one of three homo-polymers with aromatic side groups: poly-L-tryptophan (PTrp), poly-L-tyrosine (PTyr), and polystyrene (PS). In the above model system, PLL provides typical cations (NH_3R^+) whereas the aromatic polymers provide π systems (i.e., indole, phenol, and benzene) commonly present in biological systems. The two surfaces were mounted in the SFA and their separation was monitored through the optical interference fringes of equal chromatic order (FECO) which were further transformed into force–distance curves (see Figure S1 in the Supporting Information). Figure 1 shows cation–π interactions between the positively charged groups and tested aromatic side groups; these interactions can be affected by the presence of other types of cations (e.g. K^+, Na^+, Li^+, TEA, ACh).

Adhesive forces between PTrp and PLL are dependent on the contact time (Figure 2a). The separation distance D is

---

[*] Dr. Q. Lu,[+] Prof. H. Zeng
Department of Chemical and Materials Engineering
University of Alberta
Edmonton, AB, T6G 2V4 (Canada)
E-mail: hongbo.zeng@ualberta.ca
D. Y. X. Oh,[+] Prof. D. S. Hwang
POSTECH Ocean Science and Technology Institute
School of Environmental Science and Engineering
Pohang University of Science and Technology
Pohang, Gyeongbuk, 790-784 (Korea)
E-mail: dshwang@postech.ac.kr
Y. J. Lee, Prof. Y. S. Jho
Department of Physics
Pohang University of Science and Technology
Asia Pacific Center for Theoretical Physics
Pohang, Gyeongbuk, 790-784 (Korea)
[+] These authors contributed equally to this work.

[**] The work was supported by an NSERC discovery grant award and an NSERC RTI grant award (for a surface forces apparatus) from the Natural Sciences and Engineering Research Council of Canada (H.Z.), the National Research Foundation of Korea Grant (grant number NRF-C1ABA001-2011-0029960), and the Marine Biomaterials Research Center grant from the Ministry of Land, Transport and Maritime Affairs, Korea (D.S.H.), and partially supported by a grant NRF-2012R1A1A2009275 and the Supercomputing Center/Korea Institute of Science and Technology Information with supercomputing resources including technical support (Y.S.J.).

Supporting information for this article is available on the WWW under http://dx.doi.org/10.1002/anie.201210365.

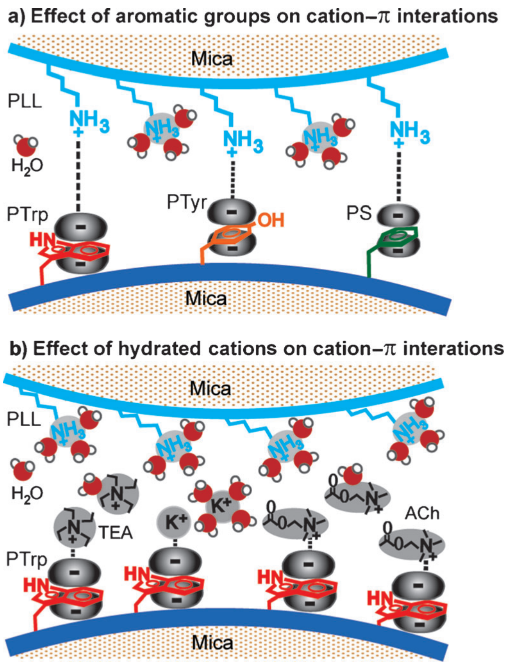

Figure 1. Aqueous cation–π interaction schemes. a) Effect of aromatic groups. Cation–π interactions occur between positively charged side groups of PLL and aromatic side groups of polymers (PTrp, PTyr, or PS). The amine group should be perpendicular to the π-electron-rich plane of the benzene ring to achieve an efficient cation–π interaction. Density differences in the π-electrons of the side phenyl groups in PTrp, PTyr, and PS could result in different cation–π interaction strengths. b) Effect of hydrated cations (K^+, TEA, and ACh). The presence of hydrated cations (K^+, TEA, and ACh) could compete with PLL cations by interacting with the aromatic groups. The ions are well solvated or hydrated in aqueous solution which results in a desolvation penalty for cation–π interactions.

referred to the contact position between mica and mica coated with aromatic polymers in air. Reversible and robust adhesion F_{ad}, similar to Fe^{3+}/DOPA complex[10c] and 1/5 times biotin/avidin interaction,[10d] was observed between PTrp and PLL during separation (Figure 2a). It was found that the adhesion energy per unit area[10a] $W_{ad} = F_{ad}/1.5\pi R$ slightly increased from 1.9 to 2.1 mJ m^{-2} with increasing contact times from 2 to 40 minutes, respectively. Such slight time-enhanced adhesion can be attributed to several factors, such as molecular reorientation (so called "en face"),[11a] removal of competing cations,[11b] and desolvation.[11c] The confined PLL-PTrp thickness did not change significantly over contact time which suggests that the contribution of conformational change of the adsorbed PLL layer might be limited. The above adhesion values were much higher than the salt bridge energy between two oppositely charged electrolyte multilayer of PLL and poly-L-glutamic acid (PGA) in aqueous solutions measured by SFA previously,[12] which suggests that the adhesion measured between PTrp and PLL arises from the cation–π interaction and is consistent with the theoretical prediction by Gallivan and Dougherty[1h] that a cation can bind more strongly to a hydrophobic aromatic group through cation–π interaction than to a hydrophilic anion by a salt bridge in aqueous solution.

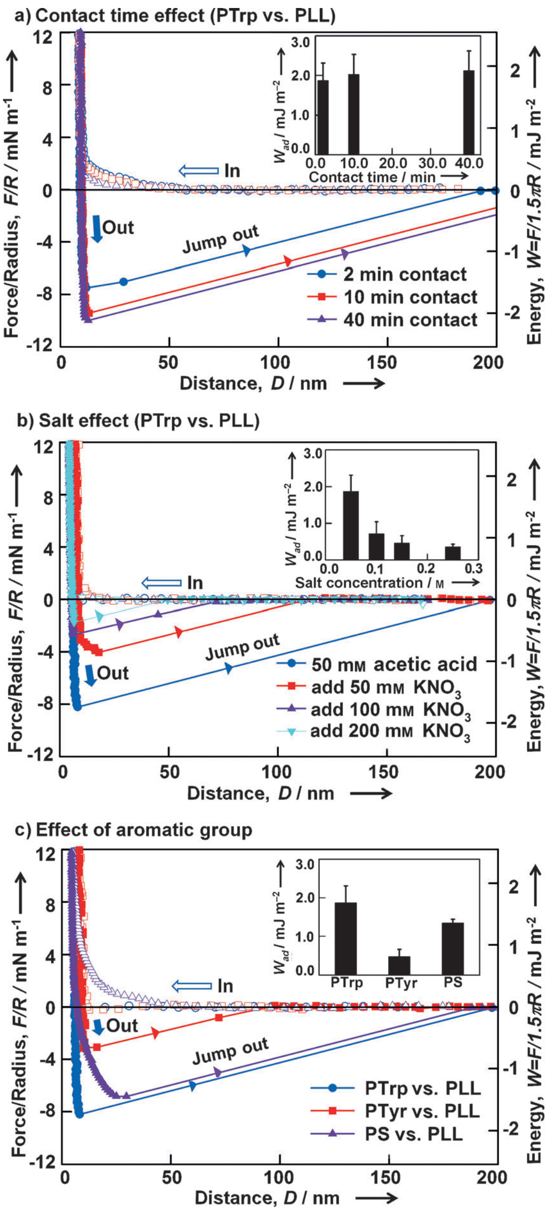

Figure 2. Typical force–distance profiles (F/R vs. D) and corresponding interaction energies ($W = F/1.5\pi R$) between PTrp and PLL films in aqueous buffer as a function of contact time, KNO_3 concentration, and aromatic groups. a) The effects of contact time were examined by keeping the two surfaces in contact for 2, 10, and 40 minutes in 0.05 M HAc, pH 3.0. b) Salt effects at a contact time of 2 minutes were examined in 0.05 M acetic acid, pH 3.0 with the addition of different amount of KNO_3 (0, 0.05, 0.1 and 0.2 M). c) Effects of aromatic groups were examined by comparing PLL interactions with aromatic polymers (PTrp, PTyr, and PS) in 0.05 M acetic acid, pH 3.0, at a contact time of 2 minutes. D is the distance between the bare mica layer and an aromatic polymer layer. W_{ad} is the adhesion energy per unit area ($W_{ad} = F_{ad}/1.5\pi R$). The insets show the corresponding adhesion energy W_{ad} (mean ± standard deviation, $n \geq 3$) dependence.

With increasing KNO_3 concentration from 0 to 0.2 M, the adhesion between PTrp and PLL decreased from about 2.0 to about 0.36 mJ m^{-2} in 0.05 M acetic acid, pH 3.0 (Figure 2b). The increased KNO_3 concentration could 1) compress the electrical double layer of the PLL surface and thus weaken the electrostatic force, and/or 2) weaken the cation–π interaction between PLL and PTrp through the competition of K^+ ions with the cations on PLL for interaction with indole groups on the PTrp surface. The Debye length (thickness) of the electrical double layer is given by $\kappa^{-1} = 0.304/\left(\sqrt{[\mathrm{KNO_3}]+[\mathrm{HAc}]}\right)$ nm and the electrostatic interaction energy W_{dl} does not significantly change under the salt concentration range (0.05–0.25 M) based on the Hogg–Healy–Fuerstenau (HHF) model.[13] However, the inset of Figure 2b shows that the adhesion decays quickly with an increase in K^+ ions, indicating that other interaction mechanisms (e.g., cation–π interactions between K^+ ions and indole groups) play a more important role. The hydration radius of a K^+ ion is similar to that of a NH_4^+ ion and so as the cation-π binding energy, whereas alkyl-NH_3^+ is less solvated[14] and has a lower desolvation penalty than hydrated NH_4^+ and K^+ ions. The cation–π binding capabilities of K^+, NH_4^+, and alkyl-NH_3^+ are similar, and K^+ ions will compete with the positively charged functional groups on PLL, reducing the adhesion between PLL and PTrp. There was no significant difference in adhesion between PLL and PTrp when the solution pH was increased from 3.0 to 6.8 (Figure S2), which is reasonable as the charges on PLL amine groups (pK_a 10.79) are not expected to change much in this pH range (3–7). The confined PLL-PTrp thickness slightly increased from about 8.0 nm (pH 3.0) to about 12.0 nm (pH 6.8), which is qualitatively consistent with the increased PLL hydrodynamic radius measured at higher pH by dynamic light scattering measurements (Figure S3).

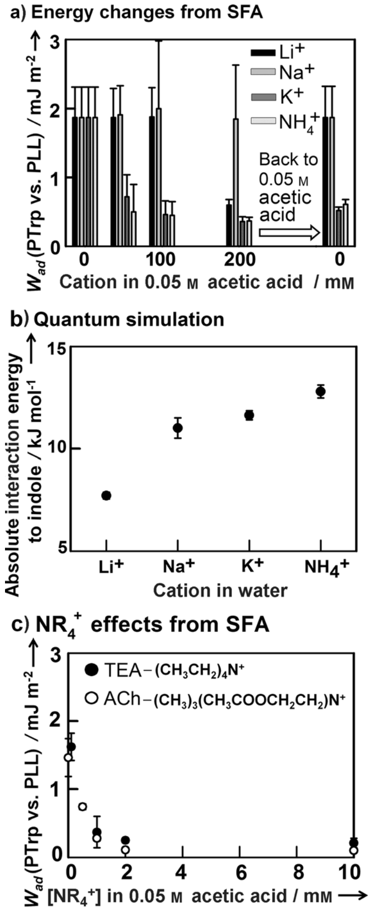

Figure 3. Cation effects on aqueous cation–π interactions. a) Energy changes between PTrp and PLL films in buffer after the addition of cations (Li^+, Na^+, K^+, or NH_4^+) obtained from SFA measurements in 0.05 M acetic acid, pH 3.0, with MNO_3 ($M^+ = Li^+$, Na^+, K^+) or NH_4Ac concentrations of 0, 0.05, 0.1, and 0.2 M, at a contact time of 2 minutes. To examine the reversibility of metal ion effects, solutions were switched from 0.2 M MNO_3 or NH_4Ac to 0.05 M acetic acid, pH 3.0 by sufficient rinsing, and the adhesion energies were measured again. b) Absolute minimum interaction energies between indole (C_8H_7N) and the cations Li^+, Na^+, K^+, and NH_4^+ in solution based on quantum simulation at an equilibrium distance between indole and cations separated along the C6 axis of 0.316, 0.29, 0.32, 0.3 nm, respectively. c) Quaternary ammonium (NR_4^+) ion effects (0 to 10 mM) on the interactions between PTrp and PLL films in aqueous solutions of 0.05 M acetic acid, pH 3. Results are shown as mean ± standard deviation ($n \geq 3$).

The adhesion strengths between PLL and the three aromatic polymers follow the order PTrp > PS > PTyr (Figure 2c). These results are qualitatively consistent with previous results which demonstrated that the strength of cation–π interactions for different aromatic groups in the gas phase follows the order of indole > benzene ≈ phenol.[1a,j,15] Compared to the very small difference observed in the gas phase, the cation–π interaction strength of benzene is over twice that of phenol in aqueous solution. Such difference might be caused by the different polymer backbone structures of PS and PTyr (aliphatic vs. peptide).

The mono-valent cations Li^+, Na^+, K^+, and NH_4^+ showed different impacts on the adhesive interactions between PTrp and PLL in 0.05 M acetic acid (Figure 3a). In contrast to the remarkable reduction in the PTrp–PLL adhesion caused by the addition of KNO_3 and NH_4Ac, the presence of $LiNO_3$ did not cause a significant decrease in the PTrp–PLL adhesion until a concentration of about 0.2 M $LiNO_3$ was reached. The presence of $NaNO_3$ (0.05–0.2 M) did not result in a significant decrease in the PTrp–PLL adhesion. Figure 3a also shows that the adhesion between PTrp and PLL fully recovered to the initial strength after switching the buffer containing 0.2 M $LiNO_3$ or $NaNO_3$ back to 0.05 M acetic acid, pH 3.0 by sufficient rinsing. However, no significant adhesion recovery was observed for the cases of KNO_3 and NH_4Ac (Figure 3a), indicating that K^+ and NH_4^+ ions bind more strongly than Li^+ and Na^+ ions to the PLL surface.[16] The adhesion energy of a mono-valent cation to an aromatic group depends mainly on the hydration radius of the cation and is expected to decrease as the hydrated ion radius increases because the larger hydration shell screens the cation–π interaction. Thus, the adhesion energy to aromatic groups is expected to follow the order $NH_4^+ \approx K^+ > Na^+ > Li^+$. The "binding" strength of hydrated cations to PTrp follows the order NH_3R^+, NH_4^+, $K^+ > Li^+$, Na^+ in aqueous solutions,[2b,1k] whereas in the gas phase the order is $Li^+ > Na^+ > K^+$, $NH_4^+ \geq NH_3R^+$.[1g,11c,16] The above results are consistent with the theoretical prediction by Kumpf and Dougherty.[1k]

To further understand the cation–π interaction mechanisms, interaction energies between indole and the cations Li^+, Na^+, K^+, and NH_4^+ in solution were calculated using quantum simulation.[17] As shown in Figure 3b, the affinity of the cations to indole follows the order $Li^+ < Na^+ < K^+ <$

NH_4^+, consistent with previous simulations.[1k] Regardless of the differences in the hydration shell radii of Li^+, Na^+, K^+, and NH_4^+ (0.382, 0.358, 0.331, and 0.331 nm, respectively), equilibrium is established at about 0.3 nm. The result implies that although smaller ions (i.e., Li^+, Na^+) have stronger charge–quadrupole interactions, they have to pay larger desolvation energy costs, which enables larger ions (i.e., K^+ and NH_4^+) to have stronger binding affinities like Hofmeister series. This result is consistent with previous investigation that solvation of a metal ion decreases its interaction energy with a π system.[18]

Based on the simulated cation–π interaction energy (around 13 $kJ\,mol^{-1}$ for indole–NH_4^+) and the adhesion energy measured by SFA (around 1.9 $mJ\,m^{-2}$ for PTrp–PLL), there was one effective cation–π interaction found for an area of 3.4 nm × 3.4 nm assuming that the adhesion measured was dominated by the cation–π interaction. Such cation–π interaction efficiency between two polymer-anchored surfaces is reasonable considering the following factors. First, the distance is about 0.38 nm between the neighboring π systems (Trp to Trp) in PTrp ($[NH\text{-}C(Trp)\text{-}CO]_n$) or between the neighboring cation systems (NH_3R^+ to NH_3R^+) in PLL ($[NH\text{-}C(NH_3R^+)\text{-}CO]_n$), which is the contour length of a peptide bond. The interaction efficiency between the functional groups is limited by their separation distance, alignment, and diffusion. Second, in contrast to interactions between small molecules, many of the cation–π interactions between side groups of polymers cannot achieve an optimized bond distance because of entropic (or steric) restrictions. Third, the cation–π interaction is highly orientation dependent, that is, the cations (NH_3R^+) should be perpendicular to the electron-rich plane of the benzene rings (Trp) to initiate effective cation–π interactions.[11b] Such orientation-sensitivity can significantly decrease the efficiency of cation–π interactions between polymer surfaces.

To compare the "binding" capability of NR_4^+, NH_4^+, K^+, and better understand the cation–π interactions related to important biological phenomena (i.e., potassium channel blockers, nicotinic acetylcholine receptors), quaternary ammonium NR_4^+ such as a potassium channel blocker (TEA = $(CH_3CH_2)_4N^+$) and a neurotransmitter (ACh = $(CH_3)_3(CH_3COOCH_2CH_2)N^+$) was introduced into the solution and competed with the interaction between PTrp and PLL. The addition of small amounts of TEA or ACh (< 0.5 mM) dramatically decreases the adhesion between PTrp and PLL (Figure 3c). Such blocking effects are much more significant than the addition of the same concentrations of NH_4^+ or K^+ ions, possibly because the quaternary ammonium ion binds aromatic groups with a higher affinity than K^+, suggesting a "binding" order of $NR_4^+ > NH_3R^+ > NH_4^+ \approx K^+$ to PTrp under physiological conditions. Thus, the SFA results confirmed that quaternary ammonium TEA and ACh, a potassium channel blocker and a neurotransmitter, respectively, bound more effectively to aromatic residues under physiological conditions than NH_4^+, K^+, and Na^+ ions.

SFA measurements and theoretical simulations confirm that cation–π interactions in aqueous media depend on the type and concentration of positively charged ions (TEA, ACh, Lys^+, NH_4^+, K^+, Li^+, and Na^+) and the type of aromatic side groups (indole, phenol, and benzene) present in the solution (Figure 1). The cation–π interaction mechanisms obtained in this study offer insights into molecular interactions involving cations and aromatic groups in living cells, such as self-assembly of biomacromolecules, molecular sensing, and signal transduction, as well as development of novel carbon-based energy materials (e.g., based on the cation–π interactions between Li^+ ions and the graphite π electron system).

Received: December 30, 2012

Keywords: cations · cation–π interactions · noncovalent interactions · potassium channel · surface forces apparatus

---

[1] a) J. C. Ma, D. A. Dougherty, *Chem. Rev.* **1997**, *97*, 1303 – 1324; b) D. A. Dougherty, *Science* **1996**, *271*, 163 – 168; c) G. Waksman, D. Kominos, S. C. Robertson, N. Pant, D. Baltimore, R. B. Birge, D. Cowburn, H. Hanafusa, B. J. Mayer, M. Overduin, M. D. Resh, C. B. Rios, L. Silverman, J. Kuriyan, *Nature* **1992**, *358*, 646 – 665; d) N. D. Zacharias, A. Dougherty, *Trends Pharmacol. Sci.* **2002**, *23*, 281 – 287; e) L. M. Salonen, M. Ellermann, F. Diederich, *Angew. Chem.* **2011**, *123*, 4908 – 4944; *Angew. Chem. Int. Ed.* **2011**, *50*, 4808 – 4842; f) P. C. Kearney, L. S. Mizoue, R. A. Kumpf, J. E. Forman, A. McCurdy, D. A. Dougherty, *J. Am. Chem. Soc.* **1993**, *115*, 9907 – 9919; g) S. Mecozzi, A. P. West, Jr., D. A. Dougherty, *J. Am. Chem. Soc.* **1996**, *118*, 2307 – 2308; h) J. P. Gallivan, D. A. Dougherty, *J. Am. Chem. Soc.* **2000**, *122*, 870 – 874; i) R. Wu, T. B. McMahon, *J. Am. Chem. Soc.* **2008**, *130*, 12554 – 12555; j) S. Mecozzi, A. P. West, Jr., D. A. Dougherty, *Proc. Natl. Acad. Sci. USA* **1996**, *93*, 10566 – 10571; k) R. A. Kumpf, D. A. Dougherty, *Science* **1993**, *261*, 1708 – 1710; l) A. S. Mahadevi, G. N. Sastry, *Chem. Rev.* **2012**, DOI: 10.1021/cr300222d.

[2] a) R. MacKinnon, G. Yellen, *Science* **1990**, *250*, 276 – 279; b) C. A. Ahern, A. L. Eastwood, H. A. Lester, D. A. Dougherty, R. Horn, *J. Gen. Physiol.* **2006**, *128*, 649 – 657; c) L. Heginbotham, R. MacKinnon, *Neuron* **1992**, *8*, 483 – 491; d) S. A. Pless, J. D. Galpin, A. Frankel, C. A. Ahern, *Nat. Commun.* **2011**, *2*, 351.

[3] a) J. D. Schmitt, C. G. V. Sharples, W. S. Caldwell, *J. Med. Chem.* **1999**, *42*, 3066 – 3074; b) N. Unwin, *Nature* **1995**, *373*, 37 – 43.

[4] E. V. Pletneva, A. T. Laederach, D. B. Fulton, N. M. Kostic, *J. Am. Chem. Soc.* **2001**, *123*, 6232 – 6245.

[5] C. Mazza, N. Auphan-Anezin, C. Gregoire, A. Guimezanes, C. Kellenberger, A. Roussel, A. Kearney, P. A. van der Merwe, A. M. Schmitt-Verhulst, B. Malissen, *EMBO J.* **2007**, *26*, 1972 – 1983.

[6] a) D. S. Hwang, H. Zeng, Q. Lu, J. N. Israelachvili, J. H. Waite, *Soft Matter* **2012**, *8*, 5640 – 5648; b) Q. Lu, D. S. Hwang, Y. Liu, H. Zeng, *Biomaterials* **2012**, *33*, 1903 – 1911.

[7] A. Ikeda, S. Shinkai, *J. Am. Chem. Soc.* **1994**, *116*, 3102 – 3110.

[8] a) X. Xiu,, N. L. Puskar, J. A. P. Shanata, H. A. Lester, D. A. Dougherty, *Nature* **2009**, *458*, 534 – 537; b) S. A. Pless, J. D. Galpin, A. P. Niciforovic, C. A. Ahern, *Nat. Chem. Biol.* **2011**, *7*, 617 – 623.

[9] a) K. Otomo, A. Toyama, T. Miura, H. Takeuchi, *J. Biochem.* **2009**, *145*, 543 – 554; b) Y. Xue, A. V. Davis, G. Balakrishnan, J. P. Stasser, B. M. Staehlin, P. Focia, T. G. Spiro, J. E. Penner-Hahn, T. V. O'Halloran, *Nat. Chem. Biol.* **2008**, *4*, 107 – 109; c) G. J. Thomas, Jr., *Biopolymers* **2002**, *67*, 214 – 225.

[10] a) J. N. Israelachvili, Y. Min, M. Akbulut, A. Alig, G. Carver, W. Greene, K. Kristiansen, E. Meyer, N. Pesika, K. Rosenberg, H. Zeng, *Rep. Prog. Phys.* **2010**, *73*, 036601 – 036617; b) J. N. Israelachvili, G. E. Adams, *Nature* **1976**, *262*, 773 – 776; c) H. Zeng, D. S. Hwang, J. N. Israelachvili, J. H. Waite, *Proc. Natl. Acad. Sci. USA* **2010**, *107*, 12850 – 12853; d) C. A. Helm, W. Knoll, J. N. Israelachvili, *Proc. Natl. Acad. Sci. USA* **1991**, *88*, 8169 – 8173.

[11] a) M. S. Marshall, R. P. Steele, K. S. Thanthiriwatte, C. D. Sherrill, *J. Phys. Chem. A* **2009**, *113*, 13628 – 13632; b) R. Amunugama, M. T. Rodgers, *J. Phys. Chem. A* **2002**, *106*, 9718 – 9728; c) J. C. Amicangelo, P. B. Armentrout, *J. Phys. Chem. A* **2000**, *104*, 11420 – 11432.

[12] Á. Kulcsár, P. Lavalle, J. C. Voegel, P. Schaaf, P. Kékicheff, *Langmuir* **2004**, *20*, 282 – 286.

[13] R. Hogg, T. W. Healy, D. W. Fuersten, *Trans. Faraday Soc.* **1966**, *62*, 1638 – 1651.

[14] Y. Marcus, A. Rashin, *Biophys. Chem.* **1994**, *51*, 111 – 127.

[15] a) C. A. Deakyne, M. Meot-Ner, *J. Am. Chem. Soc.* **1985**, *107*, 474 – 479; b) S. E. Wheeler, K. N. Houk, *J. Am. Chem. Soc.* **2009**, *131*, 3126 – 3127.

[16] A. S. Reddy, G. N. Sastry, *J. Phys. Chem. A* **2005**, *109*, 8893 – 8903.

[17] a) M. Valiev, E. J. Bylaskaa, N. Govinda, K, Kowalskia, T. P. Straatsmaa, H. J. J. Van Dama, D. Wanga, J. Nieplochaa, E. Aprab, T. L. Windusc, W. A. de Jonga, *Comput. Phys. Commun.* **2010**, *181*, 1477 – 1489; b) A. Klamt, G. Schüürmann, *J. Chem. Soc. Perkin Trans. 2* **1993**, 799 – 805.

[18] J. S. Rao, H. Zipse, G. N. Sastry, *J. Phys. Chem. B* **2009**, *113*, 7225 – 7236.